Developmental Biology **225,** 459–470 (2000)
doi:10.1006/dbio.2000.9805, available online at http://www.idealibrary.com on IDEAL®

Drosophila dec-1 Eggshell Proteins Are Differentially Distributed via a Multistep Extracellular Processing and Localization Pathway

M. Isabel Noguerón, Debra Mauzy-Melitz, and Gail L. Waring
Biology Department, Marquette University, Milwaukee, Wisconsin 53233

In *Drosophila* the multilayered eggshell forms during late oogenesis between the oocyte and the overlaying follicle cells. Proper eggshell assembly requires wild-type *dec-1* gene function. Alternatively spliced *dec-1* transcripts encode three proproteins that are cleaved extracellularly in a stage-specific manner to at least five distinct derivatives. Using polyclonal antibodies raised against fusion proteins containing different regions of the *dec-1* proteins, we have localized several *dec-1* derivatives in the assembling and completed eggshell. Although all of the *dec-1* derivatives are generated in the oocyte proximal vitelline membrane layer, they are differentially distributed in the mature egg. Some derivatives are gradually released from the vitelline membrane and become localized within distinct regions of the chorion, while others are taken up by the oocyte or become concentrated in the endochorionic spaces or cavities. The diverse distributions of the *dec-1* derivatives suggest that each derivative plays a distinct role in eggshell assembly. These results also suggest that the vitelline membrane layer, by acting as a transient storage site, may control the availability of molecules active in eggshell assembly and by extension perhaps other follicle cell products important in early embryonic pattern formation.

Key Words: **extracellular assembly; eggshell; *Drosophila;* protein trafficking; immunolocalization.**

INTRODUCTION

The assembly of organized, complex three-dimensional structures is a fundamental process that occurs in all cells and developing organisms. The assemblies of intracellular structures such as the ribosome, nuclear pore complex, and cytoskeletal networks have been the focus of several investigations. To elucidate some of the molecular strategies and mechanisms that are used to promote the assembly of extracellular structures in a developing organism we have been studying eggshell formation in *Drosophila.* The *Drosophila* eggshell is a highly organized multilayered structure that forms between the oocyte and the overlaying follicle cells during late oogenesis. Largely proteinaceous, its production involves intercellular signaling (reviewed in Morgan and Mahowald, 1996), directed cell migrations (Deng and Bownes, 1998), regulated gene expression (Cavaliere *et al.*, 1997; Orr-Weaver, 1991; Popodi *et al.*, 1988), postdepositional processing (Noguerón, 1996; Pascucci *et al.*, 1996), and the transient sequestration of selected eggshell components (Pascucci *et al.*, 1996; Trougakos and Margaritis, 1998). Produced over a 30-h period in morphologically distinct developmental stages, the *Drosophila* eggshell provides an opportunity to study extracellular assembly in a developing system which features high temporal and spatial resolution.

In *Drosophila,* eggshell structural proteins are produced and secreted by ovarian follicle cells during stages 8–14 of egg chamber development. In mature stage14 egg chambers the eggshell consists of four morphologically distinct layers: an oocyte proximal vitelline membrane, a crystalline inner chorionic layer (ICL), a tripartite endochorion, and an oocyte distal exochorion. The inner vitelline membrane layer forms during stages 8–10 while the outer chorionic layers form during stages 11–14 (Margaritis, 1985). Aside from its radial complexity, the eggshell also exhibits regional complexity. The most prominent specialized structures appear at the anterior end of the egg and include the micropyle, operculum, and dorsal appendages. The micropyle protrudes from the eggshell and allows sperm access to the oocyte plasma membrane. The operculum facilitates hatching of the larva at the end of embryogenesis, while the dorsal appendages allow submerged eggs to respire (Margaritis, 1985).

Three eggshell genes which play essential roles in eggshell assembly have been identified genetically: *sV23*, *s36*, and

0012-1606/00 $35.00

defective chorion-1 (*dec-1*). s36 protein null mutants (*cor 36*) fail to organize a tripartite endochorion (Digan *et al.*, 1979). In wild-type egg chambers s36 is synthesized during the early choriogenic stages (11–13) and is localized throughout the endochorion layer in the mature stage 14 eggshell (Pascucci *et al.*, 1996), a distribution compatible with its mutant phenotype. sV23 protein null mutants form an organized endochorion initially; however, during late stage 14 electron-dense chorionic material begins to accumulate in the vitelline membrane as the endochorion collapses (Pascucci *et al.*, 1996). Synthesized during stages 8–11, sV23 is localized in the vitelline membrane layer throughout oogenesis. This suggests that molecular events within the vitelline membrane layer play an important role in the stabilization of the outer chorion layers (Pascucci *et al.*, 1996). Both the organization and the stability of the endochorion are disrupted in *dec-1* protein null mutants. A structured endochorion framework fails to form and large aggregates of electron-dense chorion material accumulate in the space between the follicle cells and the vitelline membrane (Bauer and Waring, 1987). The aggregates eventually collapse into the underlying vitelline membrane layer during late stage 14.

The *dec-1* gene encodes multiple protein products. During stages 9–12 the *dec-1* gene produces three proproteins, fc106, fc125, and fc177, from alternatively spliced mRNAs (Waring *et al.*, 1990). The three proproteins share a 944-amino-acid N-terminus that includes a central region (332 amino acids) consisting of tandem repeats of a 26-amino-acid glutamine-rich motif. The proteins are distinguished by their C-termini. The fc106-specific C-terminus is 6 amino acids in length, the fc125 specific C-terminus is138 amino acids, and the fc177 specific C-terminus is 604 amino acids. All three proproteins are cleaved in protein-specific patterns to smaller derivatives during the latter stages of oogenesis (Noguerón and Waring, 1995). To begin to understand its essential role in eggshell assembly, we have localized *dec-1* proteins in the assembling and mature eggshell. In this paper we show that all of the *dec-1* posttranslational cleavages take place extracellularly in the vitelline membrane layer and that some of the cleaved derivatives exit the vitelline membrane layer rapidly while others exit gradually and incompletely. The distinct localization patterns of the different *dec-1* derivatives in the mature eggshell are compatible with its complex mutant phenotype and suggest that distinct molecular motifs within each derivative direct its trafficking. Their diverse distributions also suggest that the *dec-1* derivatives are functionally distinct and are likely to play different roles in the assembly and stabilization of the mature eggshell.

MATERIALS AND METHODS

Drosophila Strains

The Oregon R wild-type stock and the *dec-1* mutant alleles *fs(1)410* and *Df(1)ct*^{4b1} have been described previously (Bauer and Waring, 1987; Hawley and Waring, 1988). The *fs(1)384* and *fs(1)1501 dec-1* mutants were originally described by Komitopoulou *et al.* (1983) and further characterized by Margaritis *et al.* (1991) and Waring *et al.* (1990), respectively. The fc177 overproducing transformant line utilized in this study was created as described below.

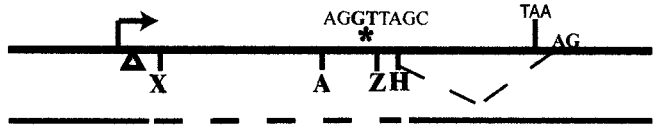

FIG. 1. Transcribed region of the fc177 transgene. The top line shows selected restriction sites and landmarks in the transcribed portion of the fc177 transgene designed to overexpress fc177 and its derivatives. X—*Xho*I, A—*Apa*I, Z—*Xba*I, and H—*Hin*dIII. The triangle below the line denotes a 173-bp intron that interrupts the *dec-1* open reading frame shortly after it begins. The positions of the 5′ donor (AG*GT*TAGC) and 3′ acceptor sites (AG) used to generate the fc125 transcript and the fc177 stop codon are indicated. The solid and dashed lines below the transcription unit indicate the regions of the transgene which were derived from genomic *dec-1* and fc177 cDNA clones, respectively.

Construction of fc177 Transgene

As shown in Fig. 1, a fc177 transgene was constructed from a mixture of fragments derived from *dec-1* genomic and cDNA clones (Waring *et al.*, 1990). The fc177 transgene included coding sequence for the fc177 transcript along with 1.9 kb of 5′ and 1 kb of 3′ *dec-1* flanking DNA. The fc177 transcript includes 5′ donor and 3′ splice acceptor sites which when used (stage 10 egg chambers) produce a smaller transcript that encodes fc125. To eliminate production of fc125 and maximize production of fc177, the fc125 5′ donor site was mutated by PCR mutagenesis. The AG*GT*TAGC shown in Fig. 1 was changed to AC*TG*CAG, creating an ectopic *Pst*I site that was used in subcloning the mutagenized PCR fragment. Briefly, an *Apa*I–*Hin*dIII subclone bearing the mutation was created in two steps. An *Apa*I–*Pst*I fragment generated by using mutated 3′ and wild-type 5′ PCR primers was subcloned into Bluescript SK(+) (Stratagene). A *Pst*I–*Hin*dIII PCR product, generated by using mutated 5′ and wild-type 3′ PCR primers, was then subcloned into the *Apa*I–*Pst*I construct. An *Apa*I–*Xba*I fragment containing the mutated donor site (*) was excised and exchanged with its wild-type counterpart in a *Xho*I–*Hin*dIII subclone (pGem 11Z vector, Promega). The *Xho*I**Xba*I insert was excised and exchanged with its wild-type counterpart in a pCaSpeR 4 P-element transformation vector that contained the *dec-1* gene along with 1.9 kb of 5′ and 1 kb of 3′ flanking DNA (G. L. Waring, unpublished). The fc177 transposon was injected into *yw* preblastoderm embryos and flies that emerged from the injected embryos were crossed with *yw* mates. Transformed flies carrying the fc177 transgene were recovered and after chromosomal linkage of the transgenes was established, homozygous "transgene" stocks were created and maintained.

Antisera

Selected open reading frames from different regions of the *dec-1* gene were subcloned into pATH expression vectors. DNA encoding 140 amino acids from the N-terminus of fc106 was used to generate

the Nfc106 serum, a segment encoding 132 amino acids from the N-terminus of s80 was used to generate the Ns80 serum, DNA encoding 254 amino acids from the C-terminus of fc106 was used for the Cfc106 serum, and a segment encoding 197 amino acids from the fc177-specific C-terminus was used for the Cfc177 serum. The generation and characterization of these rabbit polyclonal sera are described in Noguerón and Waring (1995). To follow more N-terminal sequences within the fc177-specific region, a 393-nt *Eco*RI–*Hin*dIII fragment (Fig. 2, region 4) was used to generate an additional fc177-specific antibody. While a small portion of this segment is contained in fc125/s95 (51 nt), Western blot analyses with the *Eco*RI/*Hin*dIII antiserum did not reveal reactivity with these proteins.

Fractionation of Egg Chambers

Ovaries from wild-type (Oregon R, P2 strain) females were removed in ice-cold Ringers (140 mM NaCl, 2.7 mM KCl, 0.8 mM Na_2HPO_4, 0.2 mM KH_2PO_4, pH 7.3). Stage 14 egg chambers were pooled and subjected to osmotic shock by exposure to ice-cold distilled water for 10 min. This treatment promotes separation of the chorion from the remaining vitelline membrane-bound oocyte (VMO) (Petri *et al.*, 1976). The chorions were manually removed from the egg chambers and the resulting chorion and VMO fractions were transferred to test tubes and pelleted by brief centrifugation. Pellets were resuspended in Laemmli sample buffer (Laemmli, 1970) and the soluble proteins were fractionated by SDS–PAGE. Proteins were electrophoretically transferred to PVDF membranes and processed for Western blot analysis as previously described (Noguerón and Waring, 1995). Antigen–antibody complexes were visualized indirectly by the addition of ^{125}I-protein A (New England Nuclear).

Immunolocalizations

Ovaries from wild-type or mutant females were removed in ice-cold Ringers and fixed overnight at 4°C in 100 mM phosphate-buffered saline, pH 7.4, containing 1% glutaraldehyde and either 2 or 4% formaldehyde. The fixed tissue was washed, dehydrated, and infiltrated with Lowicryl K4M resin as described in Waring (1999). Samples were polymerized in fresh resin at −25°C under UV light in a UVC2 cryo chamber (Ted Pella, Inc.). After 24 h at −25°C, polymerization under UV light was continued in the cryo chamber at ambient temperature for an additional 24 h.

For electron microscopy, thin sections (60–90 nm) cut with glass knives were mounted on Formvar-coated nickel grids. Prior to staining, grids were incubated for 60 min in 4% BSA/PBS, pH 7.4, to block nonspecific binding of the antibodies. Blocked grids were incubated either for 1.5–2.5 h at room temperature or at 4°C overnight with antibodies diluted in PBS, pH 7.4, containing 500 mM NaCl, 1% BSA, and 0.1% Tween 20 (PBS-A). Following several short washes (5 min each) in PBS, pH 7.4, containing 0.5% BSA, the grids were incubated for 1.5–2 h at room temperature in secondary antibody [15-nm gold conjugated to goat anti-rabbit IgG (Amersham Life Sciences)] diluted 1:30 in PBS-A. Washed grids were postfixed by a brief incubation in 2% glutaraldehyde (2–3 min). Following fixation the grids were washed with two changes of 0.5% BSA/PBS, pH 7.4 (5 min each) followed by two changes in Milli-Q water (<2 min each). Dried grids were stained with either a saturated uranyl acetate aqueous solution (3%) for 5 min or alcoholic uranyl acetate (5%) for 15–30 s followed by a 1-min incubation in a saturated lead citrate solution (2.5%). Grids were examined at 80 kV in a JEM 100CX II or at 75 kV in a Hitachi H-600 transmission electron microscope.

For fc177-specific immunolocalizations, the fc177 antiserum was purified prior to use by either affinity chromatography or preabsorption with whole ovaries from *dec-1* protein null mutants. For column chromatography, a bacterial fusion protein containing the fc177-specific C-terminus was electrophoretically purified and bound to activated Affi-Gel 10 matrix as described by the manufacturer (Bio-Rad Laboratories). fc177-specific antibodies were recovered from the column as described in Noguerón and Waring (1995) and stored at −20°C prior to use. Alternatively, the antiserum was preabsorbed by incubation overnight at 4°C with teased ovaries isolated from *fs(1)410 dec-1* female sterile mutants (1 μl serum/paired ovaries). Preabsorbed antibodies were used immediately.

For light microscopy, semithick sections (200–300 nm) were placed on Gold Plus slides (Erie Scientific Co.) and processed using the target retrieval Citra solution (Inno Genex, San Ramon, CA) to promote penetration of the antibodies. Prior to incubation with the antibodies, the slides were blocked for 60 min with a solution containing 5% BSA, 0.1% cold-water fish gelatin, and 10% goat serum. Unless stated otherwise, slides were washed several times in PBS, pH 7.2, containing 1% BSA followed by incubation with preadsorbed *dec-1* antibodies (1:10,000 dilution) for 1 h at room temperature or overnight at 4°C. After several brief rinses, slides were incubated for 20 min with diluted (1:50) goat anti-rabbit antibody conjugated to biotin (Inno Genex). Following several brief rinses, slides were incubated for 20 min with a streptavidin/alkaline phosphatase solution, rinsed, and incubated with fast red substrate for 20 min. Slides were viewed with a Zeiss light microscope equipped with light, phase, and fluorescence lenses. Digitized images of 35-mm slides were acquired with Scion Image software. The montages were assembled with Adobe PhotoShop software.

RESULTS

dec-1 Cleavages Are Postdepositional

To follow the distribution of *dec-1* gene products and their derivatives during development, we raised polyclonal antisera to trp-E fusion proteins containing different regions of the *dec-1* open reading frame (Noguerón and Waring, 1995). Figure 2 shows the primary translation products of the *dec-1* gene, fc106, fc125, and fc177, and the regions used for the production of antibodies used in this paper. Antisera 1–3 were directed against epitopes found in all three primary translation products. Since fc106 and its derivatives are produced and accumulate in 10- to 20-fold greater quantities than either fc125 or fc177 (Noguerón and Waring, 1995), we assumed, *a priori*, that the bulk of the immune reactivity *in situ* with these sera could be attributed to fc106 and its cleaved derivatives. The *dec-1* specificity *in situ* of all of the antisera used in this study was verified by the absence of immunoreactivity in *dec-1* protein null mutant egg chambers (*fs(1)410* or *fs(1)384*) that were processed in parallel with the wild-type egg chambers (data not shown). fc106 and fc125 accumulate in stage 9 and 10A egg chambers, a period which encompasses approximately 12 h. During stage 10B, fc106 is cleaved at its

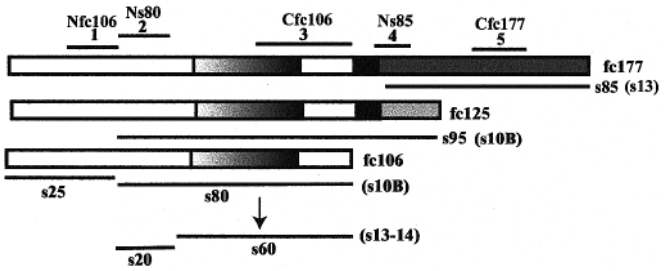

FIG. 2. Conceptual *dec-1* translation products and their processed derivatives. The boxed rectangles show the distinctive regions which comprise the three *dec-1* proproteins: fc177, fc125, and fc106. All of the proproteins contain a large central region (shaded) which consists of perfect and imperfect copies of a 26-amino-acid repeat. The black box represents a 42-amino-acid segment common to fc125 and fc177. The common region is followed by either the shaded fc177- or fc125-specific C-terminal segments. The solid lines beneath the proproteins denote their cleaved derivatives. The N-terminus of s80 has been determined by N-terminal sequencing (Waring *et al.*, 1990). The positions of the other N-termini are estimates based on the sizes and immune reactivities of the cleaved products. The stages at which the cleavages occur are indicated at the right in parentheses. Not shown are s25-, s20-, and s60-like derivatives of fc177 which have been detected in late stage *fs(1)410* egg chambers carrying the fc177 transgene (D. Mauzy-Melitz, unpublished). The lines above the fc177 proprotein indicate the regions used for the production of the *dec-1* antibodies. Serum 1 (Nfc106) recognizes all three proproteins and s25. Serum 2 (Ns80) recognizes all three proproteins, s80, s20, and s95. Serum 3 (Cfc106) recognizes the proproteins and the s60 and s95 derivatives. Antisera 4 and 5 (Ns85 and Cfc177, respectively) recognize fc177 and its C-terminal derivative, s85.

N-terminus to s25 and s80 while fc125 is cleaved to a 95-kDa C-terminal product, s95. To establish whether the cleavages of fc106 and fc125 occur intracellularly or extracellularly, we used the Nfc106 antiserum (Fig. 2) to determine if the proproteins accumulated within the follicle cells or in the extracellular space in stage 9 and 10A egg chambers. The light micrograph in Fig. 3A shows intense reactivity around the entire oocyte in an early wild-type stage 10 egg chamber. In addition to an extracellular location, the distribution suggests that fc106 is produced by all of the follicle cell subpopulations, including those that are involved in the elaboration of regional specializations at the anterior and posterior poles. Reactivity in the micropylar region of stage 12 egg chambers (Fig. 3B) is consistent with this interpretation. Immunoelectron microscopy of stage 10A egg chambers (Fig. 3C) confirmed that fc106 is found between the oocyte and the overlying follicle cells in the region where the vitelline membrane is forming.

To separate the reactivities of fc106 and fc125 we made use of *dec-1* mutant egg chambers. The deficiency chromosome, *Df(1)ct*^{4b1}, contains a breakpoint that falls in the *dec-1* transcription unit near the beginning of the fc177-specific open reading frame (Hawley and Waring, 1988). The deficiency chromosome produces near wild-type levels of fc106 and its derivatives but fails to produce either fc125 or fc177 or their derivatives (Noguerón and Waring, 1995; Waring *et al.*, 1990). The immunofluorescent staining pattern of early stage 10 egg chambers from females heterozygous for the deficiency chromosome and a *dec-1* null mutation, *fs(1)410*, was indistinguishable from the wild-type pattern (data not shown). These results confirmed that fc106 is constitutively secreted and that its temporally regulated cleavage to s80 and s25 occurs within the vitelline membrane.

As mentioned previously, fc125 is a minor *dec-1* product in wild-type egg chambers. To facilitate its visualization and distinguish it from fc106, we have utilized a *dec-1* mutant, *fs(1)1501*, which overproduces fc125. In *fs(1)1501* mutants, the 3′ splice acceptor site used to generate fc106 mRNA is mutated; efficient use of the alternative fc125 3′ splice acceptor site yields fc125 mRNA and protein in amounts comparable to those of fc106 in wild-type egg chambers. fc106 is not produced in *fs(1)1501* mutants (Waring *et al.*, 1990; Noguerón and Waring, 1995). The distribution of fc125 in *fs(1)1501* mutants likely reflects its distribution in wild type as the general structural features of *fs(1)1501* and wild-type eggshells are similar (Komitopoulou *et al.*, 1983) and processing of the fc125 protein is normal in *fs(1)1501* (Noguerón and Waring, 1995). Furthermore, overexpression of fc125 does not interfere with the production of a functional eggshell since *fs(1)1501/*

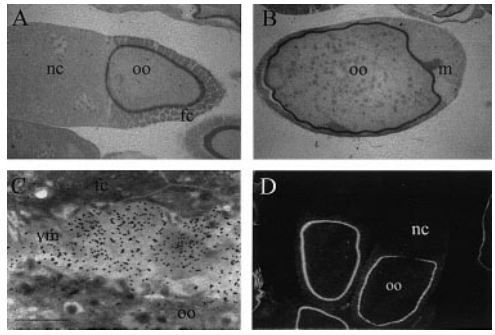

FIG. 3. Immunolocalization of fc106 and fc125. (A) Bright-field image of a section through an early stage 10 egg chamber reacted with the Nfc106 serum showing staining in the region between the follicle cells and the oocyte. The nurse cells which occupy more than one-half of the chamber are to the left (nc); the oocyte (oo) is surrounded by follicle cells (fc). (B) A bright-field image of a section through an early stage 12 egg chamber reacted with the Cfc106 serum showing reactivity in the micropyle (m). Reactivity in the micropyle was also observed with the Nfc106 serum at stage 11 (not shown). (C) Transmission electron micrograph of a sectioned early stage 10 egg chamber reacted with the Nfc106 serum (1/500 dilution) showing the accumulation of gold particles in the region where the vitelline membrane (vm) is forming. (D) An immunofluorescent image of a sectioned early *fs(1)1501* stage 10 egg chamber reacted with Nfc106 serum. The scale bar in (C) represents 1 μm.

Df(1)ct^{4b1} heterozygotes are fertile and display wild-type eggshell morphology despite the elevated levels of fc125. The extracellular localization of fc125 in early stage 10 egg chambers from homozygous *fs(1)1501* females (Fig. 3D) indicates that like fc106, fc125 is constitutively secreted.

Trafficking of s25 to the Chorionic Layers during Late Oogenesis

In *dec-1* null mutants the endochorion fails to organize into a tripartite structure and endochorion material collapses into the vitelline membrane layer in late stage 14 egg chambers. Abnormal chorion morphology has been previously associated with loss of both vitelline membrane (Pascucci *et al.,* 1996) and chorion structural proteins (Digan *et al.,* 1979). fc106 is localized in the vitelline membrane. Since there is precedent for transient storage of chorion proteins in the vitelline membrane layer during the early choriogenic stages (11–13) (Pascucci *et al.,* 1996; Trougakos and Margaritis, 1998), we were interested in following the distribution of the fc106 cleavage products, s25 and s80.

After stage 10, s25 is the only fc106 derivative that is recognized by the Nfc106 antiserum (Fig. 2) used in this study. Since fc125 does not generate stable N-terminal derivatives as it is cleaved (Noguerón and Waring, 1995), cross reactivity with fc125-related products is not problematic after its cleavage during stage 10B. Although much less abundant, reactivity with fc177 (stages 11–12) or its N-terminal derivative(s) (stages 12–14) cannot be excluded. Previous studies have indicated at least a 10-fold reduction in the accumulation of fc177 relative to fc106 (Hawley and Waring, 1988; Waring *et al.,* 1990). Sectioned egg chambers often display a pronounced separation between the vitelline membrane and the forming chorion layers in late choriogenic egg chambers. The separation is an artifact of fixation (Margaritis, 1985) but facilitates differentiation of the vitelline membrane and chorion layers at both the light and the EM levels. Figure 4 shows changes in the distribution of the Nfc106-reactive epitopes during the choriogenic stages. Transmission electron microscopy of wild-type stage 12 egg chambers showed immunogold labeling throughout the vitelline membrane and in the region of the forming chorion (Figs. 4A and 4B). In stage 14 egg chambers light microscopy revealed intense immunofluorescent staining in the vitelline membrane and chorion layers of the main-shell (Fig. 4C), anterior (Fig. 4D), and posterior pole regions (not shown), as well as in the micropyle (Fig. 4E). In some sections the reactivity in the chorion was split into two layers (Fig. 4D). The split likely reflects regions where the ICL has detached from the endochorion floor (Margaritis, 1985). Intense particulate staining was also observed in the oocyte of stage 14 egg chambers (Figs. 4C and 4D). The reactivity in the oocyte was not observed during the early choriogenic stages (11–13) (data not shown), suggesting that a redistribution of reactive epitopes to the oocyte occurs late during oogenesis. Electron micrographs of late stage 14 egg chambers show immunogold particles distributed throughout the roof, pillars, and floor of the endochorion layer (Fig. 4F). Gold particles were also localized within the ICL (Fig. 4G) and differentially concentrated along the oocyte distal surface of the vitelline membrane (Fig. 4H). The presence of a *dec-1* product in the ICL is consistent with defects in the crystalline structure of the ICL previously reported for the *fs(1)384 dec-1* mutants (Margaritis *et al.,* 1991).

To verify the identity of the reactive species we again made use of *dec-1* mutant egg chambers. Stage 14 egg chambers from females heterozygous for the *Df(1)*^{4b1} chromosome and the *dec-1* null mutation, *fs(1)410*, show structured eggshells that retain immunofluorescent staining in the vitelline membrane and chorion layers (data not shown), a result compatible with s25 staining. Conversely, staining of the oocyte was not detected in late stage *Df(1)ct*^{4b1}*/fs(1)410* egg chambers, suggesting that staining of the oocyte in the wild-type egg chambers was due to an N-terminal derivative of fc177. The immunofluorescent staining pattern of *fs(1)1501* stage 14 egg chambers was consistent with this interpretation. In *fs(1)1501* mutants, fc106 and its derivatives are not produced; however, fc177 and its derivatives are produced at or slightly above wild-type levels (Noguerón and Waring, 1995). Immunofluorescent staining was readily apparent in the oocytes of *fs(1)1501* stage 14 egg chambers (data not shown). The comparable intensity of the oocyte stain in wild-type and *fs(1)1501* mutant egg chambers is compatible with a fc177 derivative.

Unlike s25, s80 appears to be retained in the vitelline membrane layer as choriogenesis progresses. The distribution of s80 can be followed prior to its cleavage in late stage 13 egg chambers with either the Ns80 or the Cfc106 antiserum. When reacted with the Ns80 antiserum (serum 2—Fig. 2) stage 11 egg chambers showed an even distribution of gold particles throughout the vitelline membrane layer (see Fig. 7A). The even distribution persisted into stage 13 egg chambers. The absence of Ns80-reactive epitopes aside from the vitelline membrane during the early and midchoriogenic stages suggests that the cleavage of s80, like that of its precursor fc106, occurs within the vitelline membrane layer.

Differential Trafficking of s80 Derivatives to the Chorion and Oocyte

Cleavage of s80 in the vitelline membrane in late stage 13 and early stage 14 egg chambers yields two proteins, an N-terminal derivative of approximately 20 kDa (s20) and a 60-kDa C-terminal product, s60 (Fig. 2). This cleavage occurs when the endochorion is organizing into a tripartite structure. Since the chorion fails to become organized in *dec-1* mutants we previously postulated that s60 might be required for these later assembly events (Bauer and Waring, 1987). *A priori* one might expect that a protein with an essential role in organizing endochorion structure would be

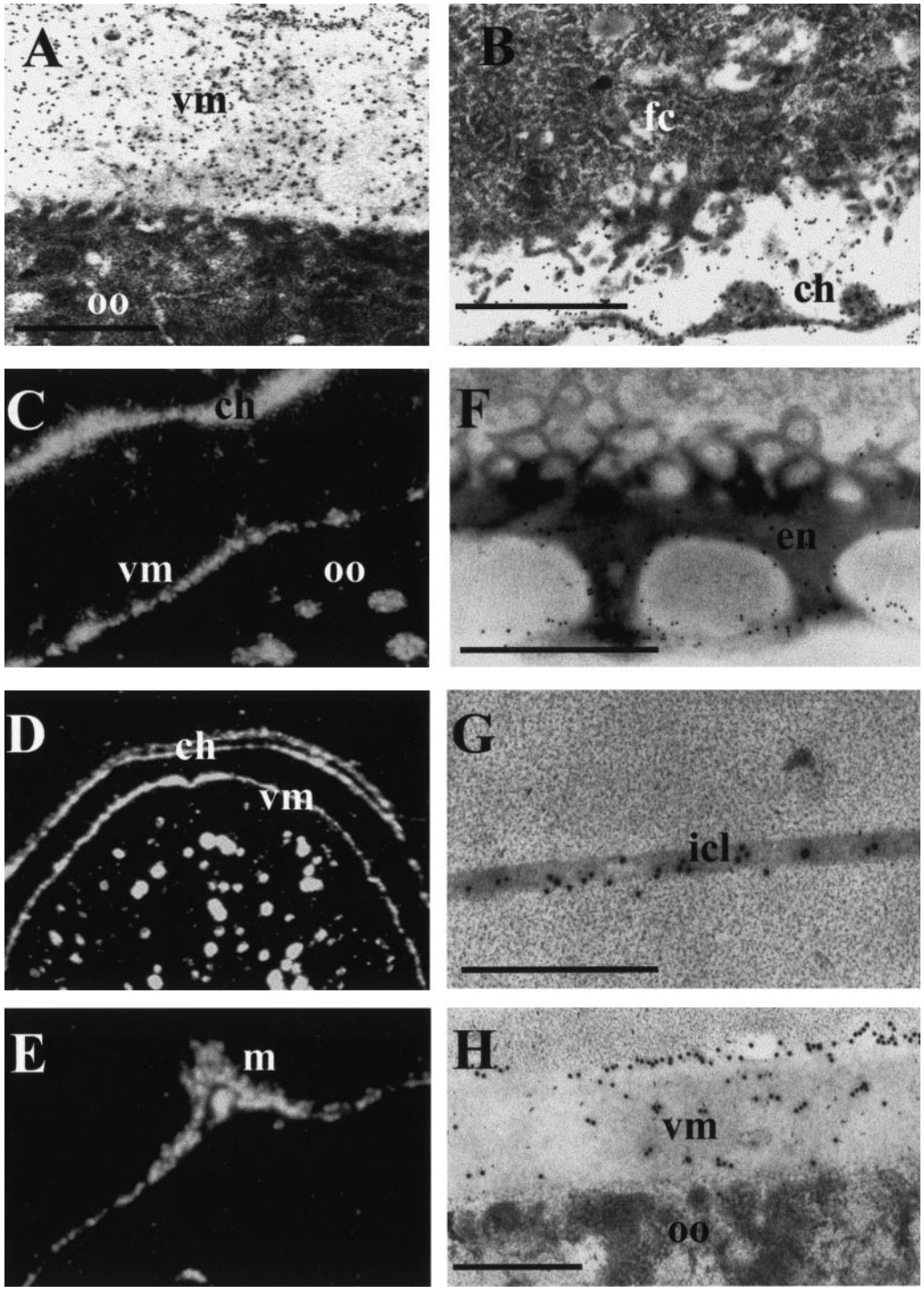

FIG. 4. Relocalization of the s25 derivative to the chorion layers during late oogenesis. (A, B) Electron micrographs of sectioned stage 12 egg chambers reacted with a 1/500 dilution of the Nfc106 antisera showing gold particles distributed throughout the vitelline membrane (vm) (A) and regions of the forming chorion (ch) (B). (C, D, E) Immunofluorescent images of sectioned stage 14 egg chambers reacted with Nfc106 serum (oo—oocyte, ch—chorion, vm—vitelline membrane, m—micropyle). (C) Main-shell region; (D) anterior region of egg chamber showing a split in the chorion layers; (E) chorion component of the micropyle. (F, G, H) Immunogold staining of the eggshell layers from sectioned stage 14 egg chambers reacted with a 1/500 dilution of Nfc106. (F) Endochorion (en), (G) inner chorionic layer (icl), and (H) vitelline membrane (vm). The scale bar in (A, B, F) represents 1 μm and in (G, H) 0.5 μm.

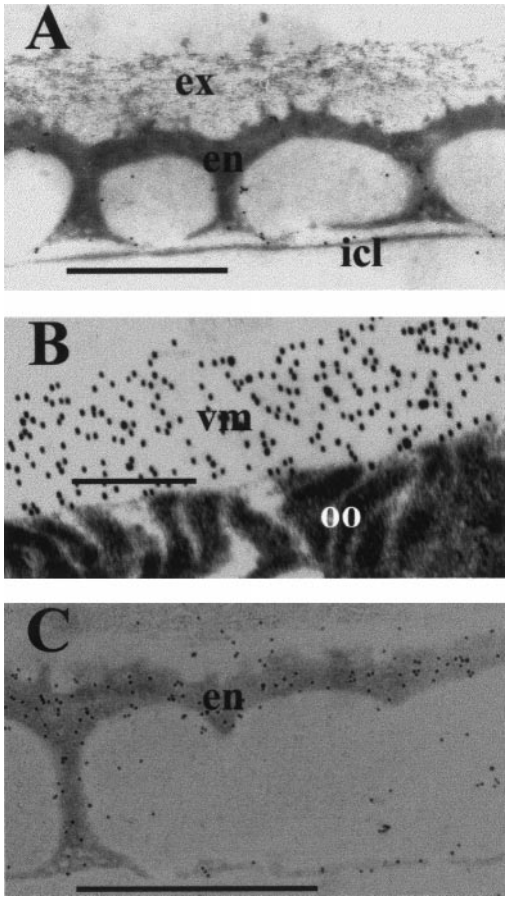

FIG. 5. Multilayered distribution of the s60 derivative in stage 14 eggshells. Immunogold staining of chorion layers (A) and vitelline membrane (B) of a stage 14 egg chamber processed as described under Materials and Methods and stained with a 1/100 dilution of purified Cfc106 antiserum. (C) Same as (A) except the ovary was fixed for 60 min in glutaraldehyde/formaldehyde rather than overnight. The scale bars in (A) represent 1 μm and in (B) 0.5 μm. ex—exochorion, en—endochorion, icl—inner chorion layer, vm—vitelline membrane, oo—oocyte.

localized in the chorion layer. Although s80, its precursor, is restricted to the vitelline membrane layer, the cleavage event which generates s60 may also trigger its release to the endochorion. In stage 14 egg chambers the predominant product detected by Western blot analysis with the Cfc106 antiserum (serum 3—Fig. 2) is s60. Figure 5 shows electron micrographs of late stage 14 egg chamber incubated with the Cfc106 serum. The majority of gold particles were found in the vitelline membrane (Fig. 5B). The small number of gold particles associated with the endochorion (Fig. 5A) appeared to be *dec-1* specific since chorionic material was not stained in stage 14 egg chambers from *fs(1)410 dec-1* mutants (data not shown).

Weak labeling of the chorion at best suggested that only a small fraction of s60 molecules move from the vitelline membrane to the chorion. Since glutaraldehyde can affect tissue antigenicity (Griffiths, 1993; Larsson, 1988), lightly fixed ovarian sections (60 min) were also reacted with the Cfc106 serum. Although preservation of the structure was compromised under these conditions, the density of gold particles over the roof and pillars of the endochorion (Fig. 5C) was comparable to, if not greater than, that over the vitelline membrane (data not shown). In neither case was reactivity observed over the ICL with the Cfc106 serum.

To determine how s60 distributes in an independent manner, stage 14 egg chambers were fractionated biochemically. Following osmotic shock, chorions were manually separated from the remaining VMO, and the SDS-soluble proteins from each fraction were analyzed by Western blot analysis. Figure 6A shows that more s60 was recovered in the chorion than in the VMO fraction. However, the relative amounts of s60 in the two fractions varied from experiment to experiment (e.g., Figs. 6B and 6C). Several factors may contribute to this variability. In early stage 14 egg chambers s80 is still being cleaved to s60. If s60 moves from the vitelline membrane to the chorion as development progresses, the proportion of s60 that associates with the chorion will depend upon the average developmental age of the egg chambers within the "stage 14" pool analyzed. Furthermore, s60, like other eggshell proteins, becomes covalently cross-linked into SDS-insoluble complexes during stage 14 (Noguerón and Waring, 1995) and only soluble s60 is monitored by Western blot analysis. If there are differences in the timing in which s60 becomes cross-linked in the vitelline membrane and chorion layers, then the distribution of s60 will be skewed by Western blot analysis. Nevertheless, taken together, the morphological and biochemical data indicate that both the vitelline membrane and the endochorion layers contain significant amounts of s60.

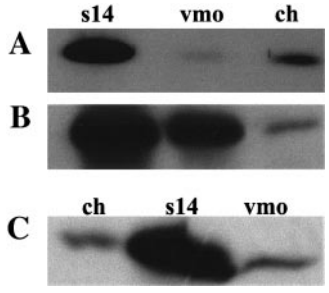

FIG. 6. Distribution of s60 in biochemically fractionated eggshells. The chorion (ch) and vitelline membrane-bound oocyte (vmo) were manually separated in stage 14 egg chambers following a brief osmotic shock. (A, B, C) Western blots of proteins in the 60 kDa range that reacted with the Cfc106 antiserum in fractions obtained from three different pools (A, B, and C) of fractionated stage 14 egg chambers. A portion of the egg chambers from each pool was removed prior to the fractionation and run in parallel (s14) to mark the position of the s60 derivative.

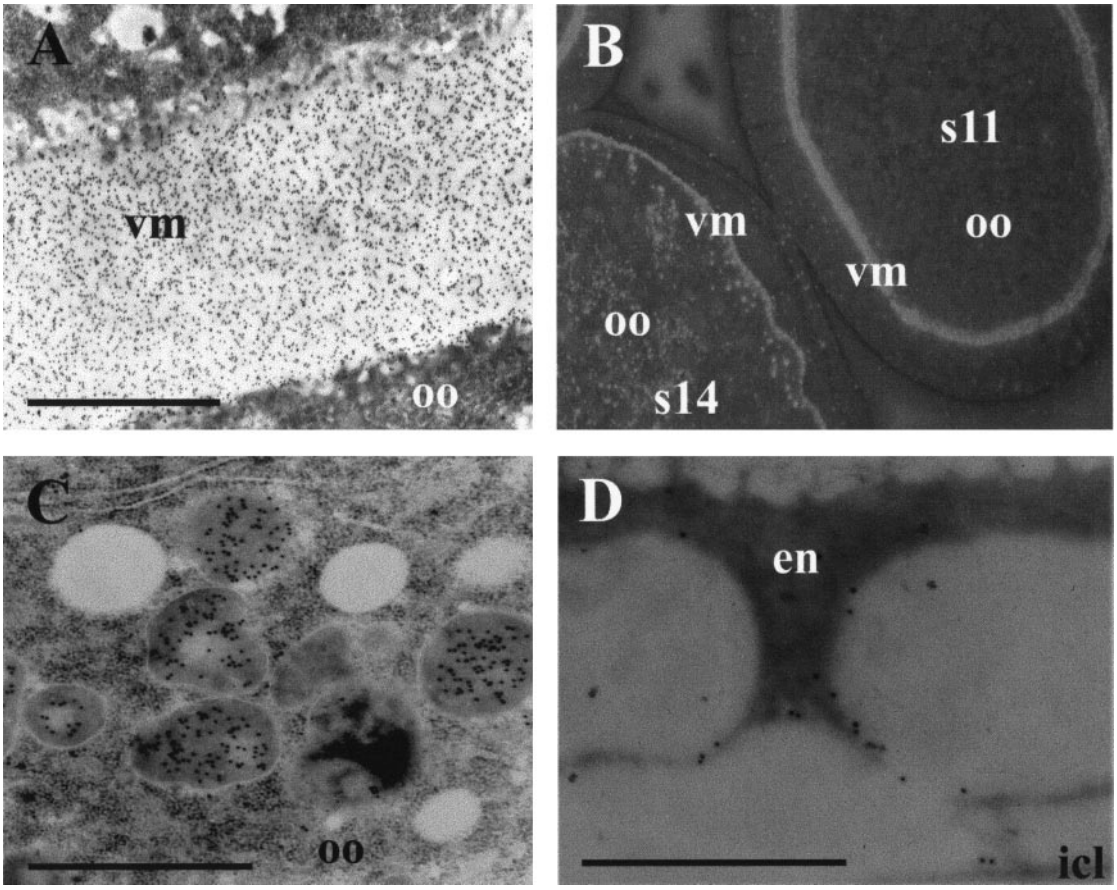

FIG. 7. Late stage uptake of s20, the N-terminal cleavage product of s80, by the oocyte. (A) Electron micrograph of a sectioned stage 11 egg chamber reacted with a 1/500 dilution of the Ns80 antiserum. (B) Immunofluorescent image of early stage 11 (s11) and early stage 14 (s14) egg chambers reacted with the Ns80 antiserum. (C, D) Immunogold staining of sectioned late stage 14 egg chambers reacted with the Ns80 antisera (1/500 dilution). (C) Immunogold particles in small membrane-bound vesicles within the oocyte (oo). (D) Scattered gold particles associated with the endochorion (en). icl—inner chorionic layer, vm—vitelline membrane. The scale bars represent 1 μm.

Contrasted with the outward movement and distribution of s25 and s60 within the eggshell, the N-terminal derivative of s80, s20, is selectively taken up by the oocyte in stage 14 egg chambers. s20 is the predominant product detected by the Ns80 antiserum in stage 14 egg chambers (Fig. 2). A 24-kDa product, s24, appears in late stage 13 egg chambers, coincident with the processing of s80 to s60. The smaller 20-kDa band prominent in stage 14 egg chambers most likely represents a modified form of s24 (Noguerón and Waring, 1995). Figure 7B shows the immunofluorescent staining patterns of a stage 11 and an early stage 14 egg chamber reacted with the Ns80 serum. As expected only the vitelline membrane stained in the stage 11 egg chamber. However, the early stage 14 egg chamber shows continuous staining in the vitelline membrane layer and punctate staining in the oocyte. Staining of the outer chorion layers was near background levels. The absence of immunofluorescent staining in the oocyte in stage 11 and early choriogenic stage egg chambers (not shown) confirmed that the relocation of the reactive epitopes was a late stage phenomenon (late stage 13, stage 14). Oocyte staining was not observed with the Cfc106 antibody (data not shown), confirming as suspected that the reactivity observed was attributable to s20, not s95. In late stage 14 egg chambers Ns80-reactive epitopes were found almost exclusively in the oocyte. Within the oocyte gold particles were associated with membrane-bound vesicles (Fig. 7C) that appeared to be more concentrated in the peripheral regions. A few gold particles were observed over the endochorion (Fig. 7D). This may reflect the distribution of the minor s95 *dec-1* component. In *fs(1)1501* egg chambers, where s95 is overproduced, the endochorion stains prominently in stage 14 egg chambers (not shown). Localization of s24/20 in the oocyte was confirmed by biochemical fractionation data. Figure 8 shows a Western blot of fractionated stage 14 egg chambers incubated with the Ns80 serum. The s24/s20 doublet was readily detected in the VMO fraction. Very weak reactivity was associated with the VMO fraction if the bulk of the

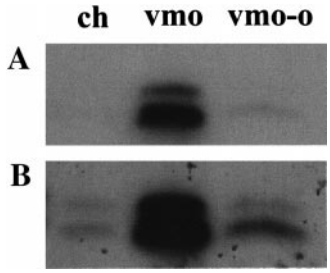

FIG. 8. Asymmetric distribution of s20 in fractionated egg chambers. Stage 14 egg chambers were separated into chorion (ch) and vmo fractions as described in Fig. 6. An independent vmo fraction from an equivalent number of egg chambers was punctured to release the oocyte contents (vmo-o). Reactive proteins in the 20 kDa range from a Western blot incubated with the Ns80 antiserum are shown (A). (B) A longer exposure of the blot shown in A emphasizing the minimal reactivity that remains in the vmo fraction after the oocyte contents have been released.

oocyte contents were released by puncturing the oocyte proper (vmo-o in Fig. 8). Taken together, these data indicate that most, if not all, of s24/20 promptly exits the vitelline membrane as it forms and is rapidly taken up by the oocyte.

s85 Concentrates within the Endochorion Spaces

Unlike fc106 and fc125, which are synthesized during the period of vitelline membrane formation, fc177 is synthesized during the early choriogenic stages (11–12). fc177 is cleaved via intermediates to a stable 85-kDa C-terminal derivative, s85, which is selectively recognized by the fc177-specific sera (4 and 5) depicted in Fig. 2. Significant levels of s85 begin to accumulate in stage 12 egg chambers; by stage 13 all of the s85 precursors have been converted into the mature form (Noguerón and Waring, 1995). When reacted with the fc177-specific sera, immunoelectron microscopy of stage 13 egg chambers revealed gold particles associated with the enlarged spaces between the pillar-like structures found at the posterior pole (not shown) and in the spaces between the pillars, the floor, and the roof of the endochorion in the main-shell region (Fig. 9A). Scattered gold particles were observed in the vitelline membrane layer (Fig. 9C). In marked contrast to its association with the endochorionic spaces in the posterior and main-shell regions, s85 was preferentially associated with electron-dense structures in the dorsal appendages (Fig. 9E). Gold particles were concentrated in pillar-like structures within the appendages and in the reticular-like network that outlines the appendages. To facilitate visualization of s85 and confirm these preliminary findings, we overexpressed fc177 in a wild-type genetic background by creating transformant lines carrying the fc177 transgene described under Materials and Methods. In wild-type egg chambers the 5.7-kb transcript encoding fc177 is produced during stages 11–12 when *dec-1* transcript accumulation *in toto* is considerably reduced relative to its peak accumulation during stages 9–10. The fc177 transgene is driven by normal *dec-1* regulatory sequences; therefore fc177 transcript production should not only be elevated, but also occur prematurely in stage 9–10 egg chambers. Since fertile transgenic lines were readily established, neither over- or premature expression of fc177 appears to be deleterious to egg chamber development. Immunoelectron microscopy indicated that as in wild type, gold particles were concentrated in the endochorionic spaces of the main-shell (Fig. 9B) and posterior pole regions (not shown) and preferentially associated with the reticulum and pillar-like structures of the dorsal appendages (Fig. 9F). As shown in Fig. 9F occasionally gold particles that appeared to track between the pillar-like structures were observed. This may indicate underlying structural heterogeneity within the spaces of the dorsal appendages. fc177-specific epitopes begin to accumulate in the dorsal appendages during the early choriogenic stages. Intense immunofluorescent staining was observed in stage 12 egg chambers in the regions associated with dorsal appendage formation (Fig. 9G). As shown in Fig. 9H, in early stage 14 egg chambers, fc177-specific epitopes extend from the base to the tips of the dorsal appendages. In addition to dorsal appendage staining, the anterior region of the stage 12 egg chamber showed intense staining in the outer chorion layer with background level immunofluorescence in the vitelline membrane layer (Fig. 9G). This contrasts with the staining pattern observed in regions where the main shell was assembling. Immunoelectron microscopy of sectioned stage 12 egg chambers showed gold particles associated with the surface of the follicle cells and the vitelline membrane in the main-shell region (data not shown). In stage 12 egg chambers eggshell development is not synchronous throughout the entire egg chamber. Elaboration of the chorion layers is more advanced in the anterior than in the main-shell or posterior regions. The different regional staining patterns observed in the stage 12 egg chamber suggest that like fc106 and fc125, fc177 initially accumulates in the vitelline membrane but either it or its C-terminal derivative, s85, is rapidly released to the assembling endochorion.

DISCUSSION

All of the *dec-1* proproteins are constitutively secreted by the follicle cells and accumulate in the vitelline membrane where they are cleaved to multiple and distinct derivatives. The *dec-1* derivatives are differentially released from the vitelline membrane layer with respect to time and amount. The release of s20 and s85 appears to be rapid and complete, while the release of s25 and s60 is gradual and incomplete. Transient storage of follicle cell products within the vitelline membrane is not without precedent. s36 and s38, major chorion proteins produced during early choriogenesis (stages 11–13), also transiently associate with the vitelline membrane (Pascucci *et al.*, 1996; Trougakos and Margaritis,

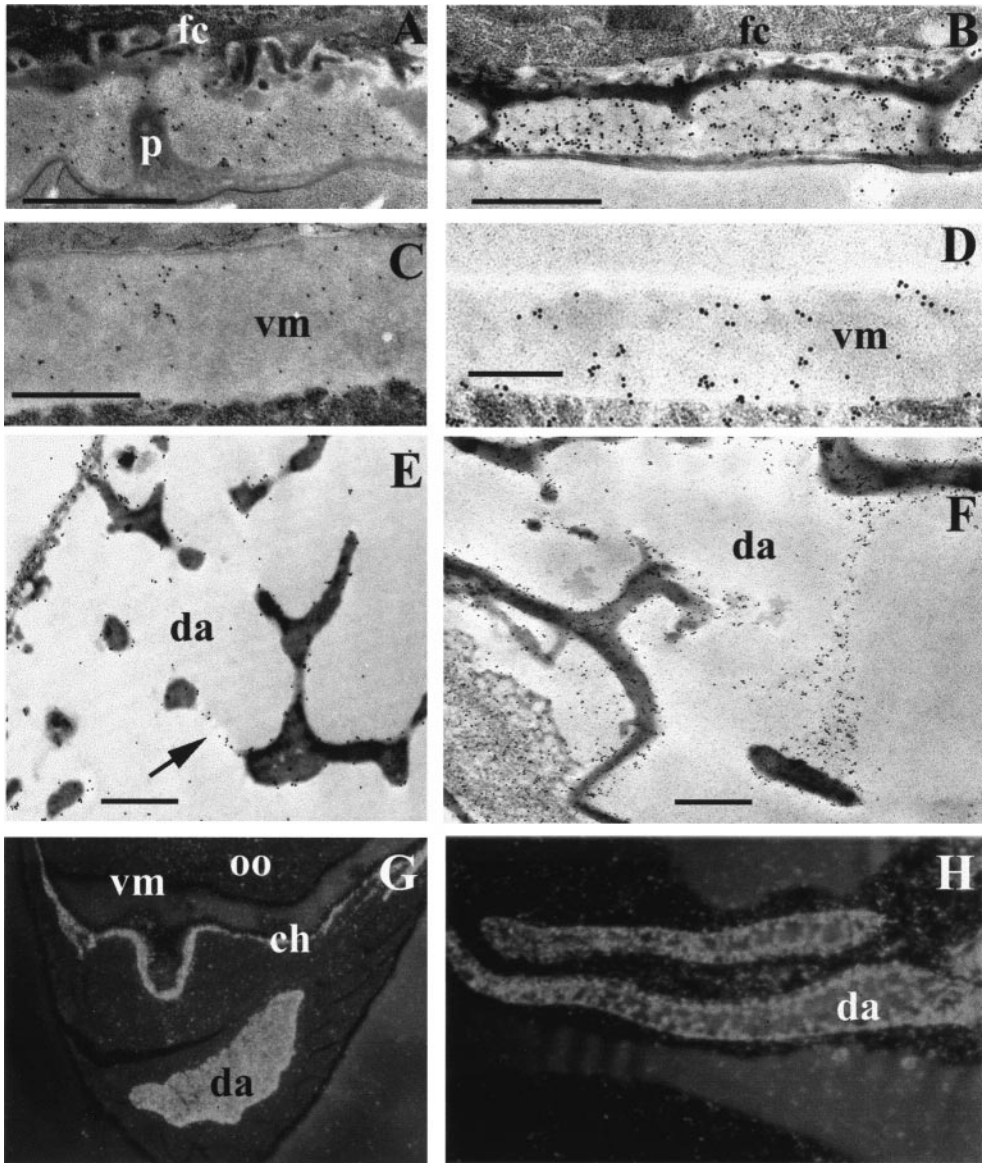

FIG. 9. The s85 C-terminal derivative of fc177 concentrates within the endochorion spaces. (A, C) Transmission electron micrographs of wild-type stage 13 egg chamber incubated with affinity-purified Cfc177 serum (1/50 dilution). (A) Gold particles between the pillars (p) of the forming endochorion; (C) underlying vitelline membrane (vm). (E) Dorsal appendage (da) from a wild-type stage 14 egg chamber incubated with preadsorbed Cfc177 (1/10,000 dilution). Gold particles tracking between the pillar-like structures (arrow) are observed occasionally. (B, D, F) Transmission electron micrographs of sectioned stage 14 egg chambers from fc177 transgenic females incubated with preabsorbed Ns85 (B, D) or Cfc177 (F) serum (1/10,000 dilution). (B) Endochorion in main-shell region; (D) underlying vitelline membrane; (F) dorsal appendage. (G, H) Immunofluorescent images of the anterior region of a sectioned stage 12 egg chamber (G) and the dorsal appendages of an early stage 14 egg chamber incubated with preabsorbed Ns85 serum. fc—follicle cell, ch—chorion, oo—oocyte, icl—inner chorionic layer. The scale bars in (A, B, E, F) represent 1 μ and in (C, D) 5 μm.

1998). Immunogold labeling of stage 12 egg chambers showed that while some s36 molecules remain near the follicle cell border in the region where the chorion assembles, most make their way to the morphologically complete vitelline membrane. In stage 14 egg chambers s36 is localized exclusively in the endochorion, hence the release of s36 from the vitelline membrane appears to be complete.

The transient sequestration and controlled release of s36 and the *dec-1* derivatives from the vitelline membrane

provides a means for temporally separating the secretion and utilization of follicle cell products. Sequestration of the chorion proteins synthesized during the early stages of eggshell formation may be necessary to accumulate threshold concentrations prior to assembly; alternatively sequestration may prevent premature or inappropriate protein–protein interactions. It is also possible that the vitelline membrane provides a surface upon which chorion subparticles assemble. A role for vitelline membrane proteins in proper chorion assembly is consistent with the sV23 protein null mutant phenotype described earlier. Perhaps in the absence of sV23 aberrant subparticles assemble which, when released, incorporate into an unstable structure that eventually collapses. While we have shown that the vitelline membrane serves as a transient storage site for several chorion components, the vitelline membrane has also been suggested as a potential storage site for follicle cell products involved in embryonic pattern formation. The activities of several follicle cell products, including nudel, pipe, and torso-like, are required during early embryogenesis, long after the follicle cells have degenerated at the end of oogenesis (Morgan and Mahowald, 1996). It has been suggested that some of these products might be stored in the vitelline membrane (Savant-Bhonsale and Montell, 1993; St. Johnston and Nusslein-Volhard, 1992).

An intriguing aspect of our immunolocalization data was the late relocation of s20 epitopes and fc177-derived N-terminal epitopes to the oocyte in stage 14 egg chambers. Endocytotic uptake of yolk proteins during the vitellogenic stages (8–10), prior to the completion of the vitelline membrane, is well documented (Engelmann, 1979; Schonbaum *et al.*, 1995); late endocytotic activity (e.g., stage 14) has not been reported. The differential and rapid uptake of the *dec-1* derivatives suggests a receptor-mediated process. While the functional significance of the uptake of these derivatives is not known, the late uptake does provide a mechanism by which the follicle cells can continue to communicate with the oocyte after the morphological completion of the vitelline membrane, a structure which has been perceived as an impenetrable physical barrier. LeMosy *et al.* (1998) have described delayed embryonic uptake of nudel, a follicle cell product essential for embryonic dorsoventral polarity. Unlike s20, during oogenesis nudel accumulates on or near the surface of the oocyte in a region that is distinct from the vitelline membrane layer, where it remains until its uptake by the early embryo.

Preliminary genetic data indicated that derivatives of at least two and most likely all three *dec-1* proproteins were necessary to assemble a functional eggshell (Hawley and Waring, 1988). The distinct localization patterns of the *dec-1* derivatives is consistent with functional multiplicity. Our light microscopic data showed that derivatives of all three *dec-1* proproteins are widely distributed regionally. Nilson and Schupbach (1998) have shown that mosaic egg chambers consisting of homozygous *dec-1* mutant follicle cell clones within a heterozygous background produce mosaic eggshells. The regions of the eggshell which overlay the mutant follicle cell clones exhibit the collapsed *dec-1* mutant phenotype. The borders of the aberrant regions align precisely with the marked *dec-1* follicle cell clones, suggesting that lateral diffusion of secreted *dec-1* proteins is minimal. Thus, the widespread distribution of the minor *dec-1* derivatives indicates that their production is not restricted to specific follicle cell subpopulations. Although both s60 and s25 display a multilayered distribution, s25 appears to be unique in its association with the ICL. Since the ICL stained only with the Nfc106 antisera we attribute this reactivity to s25. While we cannot exclude the possibility of a minor contribution from an fc177 N-terminal derivative, the lack of reactivity with the Ns80, Cfc106, and Cfc177 sera suggests that if fc177 contributes to the staining pattern it does so in the form of an s25-like product. Like s60, s95, the C-terminal derivative of the fc125 proprotein, associates with the endochorion proper (D. Mauzy-Melitz, unpublished), while s85, the C-terminal derivative of fc177, is unique in its association with the endochorionic cavities or spaces. Morphological studies have shown that the endochorionic cavities found in the main body, respiratory appendages, and posterior pole regions of stage 14 egg chambers are filled by an ill-defined flocculent material of polysaccharide nature which is secreted by the follicle cells (Margaritis, 1985). s85 is the first proteinaceous component associated with this region. It may provide a scaffold which aids in endochorion morphogenesis and/or it may be involved in its stabilization. Two distinct domains within s85 that may relate to its unique function have been revealed through an evolutionary comparison of the *Drosophila melanogaster* and *D. virilis dec-1* homologs (Badciong and Waring, unpublished). The N-terminal region of s85 contains four pairs of strictly conserved cysteine residues (CXC) within a 36-amino-acid stretch. The cysteine region is followed by a highly conserved block of 65 amino acids (93% identity) extraordinarily rich in acidic residues (30%).

The distribution of the *dec-1* derivatives in the assembling and mature eggshell raises several trafficking issues. Retention of the *dec-1* derivatives in the vitelline membrane may be the result of direct interactions with vitelline membrane proteins or the derivatives may bind indirectly as part of a protein complex. In either case, the rapid release of s20 and more than likely s85 as they are cleaved from their precursors indicates that these *dec-1* regions do not contain vitelline membrane retention sequences. The retention of the N-terminal epitopes in the form of s25 and the C-terminal epitopes in the form of s60 suggests that its precursor, fc106, is anchored at multiple sites. Finally, once the proteins are released, questions arise regarding the molecular tags that are necessary for the incorporation of s25 into the ICL, s85 into the endochorionic spaces, and s20 into the oocyte. By using a combined genetic and biochemical approach it should be possible to define the interacting motifs and proteins involved in this complex extracellular trafficking pathway and in so doing begin to understand in molecular terms how a large intricate structure such as the *Drosophila* eggshell is assembled *in vivo*.

ACKNOWLEDGMENTS

We thank Dr. Heather Owens for expert technical assistance and for use of the imaging facility at the University of Wisconsin–Milwaukee, Bill Cullinen for use of his fluorescence microscope, and members of our laboratory group for helpful discussions. This work was supported by NSF Grant IBN-920125 and NIH Grant RI5GM55952 to G.L.W.

REFERENCES

Bauer, B. J., and Waring, G. L. (1987). 7C female-sterile mutants fail to accumulate early eggshell proteins necessary for later chorion morphogenesis. *Dev. Biol.* **121,** 349–358.

Cavaliere, V., Spano, S., Andrenacci, D., Cortesi, L., and Gargiulo, G. (1997). Regulatory elements in the promoter of the vitelline membrane gene VM32E of *Drosophila melanogaster* direct gene expression in distinct domains of the follicular epithelium. *Mol. Gen. Genet.* **254,** 231–237.

Deng, W. H., and Bownes, M. (1998). Patterning and morphogenesis of the follicle cell epithelium during *Drosophila* oogenesis. *Int. J. Dev. Biol.* **42,** 541–552.

Digan, M. E., Spradling, A. C., Waring, G. L., and Mahowald, A. P. (1979). The genetic analysis of chorion morphogenesis in *Drosophila melanogaster. In* "Eucaryotic Gene Regulation ICN–UCLA Symposium" (R. Axel *et. al.,* Eds.), pp. 171–181. Academic Press, New York.

Engelmann, F. (1979). Insect vitellogenin: Identification, biosynthesis, and role in vitellogenesis. *Adv. Insect Physiol.* **14,** 49–108.

Griffiths, G. (1993). "Fine Structure Immunocytochemistry." Springer-Verlag, Berlin.

Hawley, R. J., and Waring, G. L. (1988). Cloning and analysis of the dec-1 female-sterile locus, a gene required for proper assembly of the *Drosophila* eggshell. *Genes Dev.* **2,** 341–349.

Komitopoulou, K., Gans, M., Margaritis, L., and Kafatos, F. C. (1983). Isolation and characterization of sex-linked female-sterile mutants in *Drosophila melanogaster* with special attention to eggshell mutants. *Genetics* **105,** 897–920.

Laemmli, U. K. (1970). Cleavage of structural proteins during the assembly of the head of bacteriophage T4. *Nature (London)* **227,** 680–685.

Larsson, L. I. (1988). "Immunocytochemistry: Theory and Practice." CRC Press, Boca Raton, FL.

LeMosy, E. K., Kemler, D., and Hashimoto, C. (1998). Role of Nudel protease activation in triggering dorsoventral polarization of the *Drosophila* embryo. *Development* **125,** 4045–4053.

Margaritis, L. H. (1985). Structure and physiology of the eggshell. *In* "Comprehensive Insect Physiology, Biochemistry, and Pharmacology" (G. A. Kerkut and L. I. Gilbert, Eds.), Vol. 1, pp. 153–230. Pergamon, Elmsford, NY.

Margaritis, L. H., Hamodrakas, S. J., Papassideri, I., Arad, T., and Leonard, K. R. (1991). Three-dimensional reconstruction of innermost chorion layer of *Drosophila grimshawi* and *Drosophila melanogaster* eggshell mutant *fs(1)384. Int. J. Biol. Macromol.* **13,** 247–253.

Morgan, M. M., and Mahowald, A. P. (1996). Multiple signaling pathways establish both individuation and the polarity of the oocyte follicle in *Drosophila. Arch. Insect Biochem. Physiol.* **33,** 211–230.

Nilson, L. A., and Schupbach, T. (1998). Localized requirements for windbeutel and pipe reveal a dorsoventral prepattern within the follicular epithelium of the *Drosophila* ovary. *Cell* **93,** 253–262.

Noguerón, M. I. (1996). Processing and distribution of dec-1 eggshell products in *Drosophila melanogaster. In* "Department of Biology," pp. 99. Marquette Univ., Milwaukee, WI.

Noguerón, M. I., and Waring, G. L. (1995). Regulated processing of *dec-1* eggshell proteins in *Drosophila. Dev. Biol.* **172,** 272–279.

Orr-Weaver, T. L. (1991). *Drosophila* chorion genes: Cracking the eggshell's secrets. *BioEssays* **13,** 97–105.

Pascucci, T., Perrino, J., Mahowald, A. P., and Waring, G. L. (1996). Eggshell assembly in *Drosophila:* Processing and localization of vitelline membrane and chorion proteins. *Dev. Biol.* **177,** 590–598.

Petri, W. H., Wyman, A. R., and Kafatos, F. C. (1976). Specific protein synthesis in cellular differentiation. III. The eggshell proteins of *Drosophila melanogaster* and their program of synthesis. *Dev. Biol.* **49,** 185–199.

Popodi, E., Minoo, P., Burke, T., and Waring, G. L. (1988). Organization and expression of a second chromosome follicle cell gene cluster in *Drosophila. Dev. Biol.* **127,** 248–256.

Savant-Bhonsale, S., and Montell, D. J. (1993). Torso-like encodes the localized determinant of *Drosophila* terminal pattern formation. *Genes Dev.* **7,** 2548–2555.

Schonbaum, C. P., Lee, S., and Mahowald, A. P. (1995). The *Drosophila* yolkless gene encodes a vitellogenin receptor belonging to the low density lipoprotein receptor superfamily. *Proc. Natl. Acad. Sci. USA* **92,** 1485–1489.

St. Johnston, D., and Nusslein-Volhard, C. (1992). The origin of pattern and polarity in the *Drosophila* embryo. *Cell* **68,** 201–219.

Trougakos, I. P., and Margaritis, L. H. (1998). Immunolocalization of the temporally "early" secreted major structural chorion proteins, Dvs38 and Dvs36, in the eggshell layers and regions of *Drosophila virilis. J. Struct. Biol.* **123,** 111–123.

Waring, G. L. (1999). Eggshell assembly in *Drosophila. In* "A Comparative Methods Approach to the Study of Oocytes and Embryos" (J. A. Richter, Ed.), pp. 385–396. Oxford Univ. Press, New York.

Waring, G. L., Hawley, R. J., and Schoenfeld, T. (1990). Multiple proteins are produced from the *dec-1* eggshell gene in *Drosophila* by alternative RNA splicing and proteolytic cleavage events. *Dev. Biol.* **142,** 1–12.

Received for publication March 21, 2000
Revised May 3, 2000
Accepted June 1, 2000